

K. SOLEK*, M. DZIARMAGOWSKI*

TESTS OF STEEL RHEOLOGICAL PROPERTIES AT HIGHER TEMPERATURES FOR COMPUTER SIMULATION IN ProCAST SOFTWARE

BADANIA WŁAŚCIWOŚCI WYTRZYMAŁOŚCIOWYCH STALI W PODWYŻSZONYCH TEMPERATURACH NA POTRZEBY SYMULACJI KOMPUTEROWYCH W PAKIECIE ProCAST

This paper presents the tests of properties of selected steel grades conducted at higher temperatures. The findings of these mechanical tests are presented herein in graphs and in a table. They allow us to mathematically describe a change in the stress values depending on the change in strain within the plastic range in the tested steel grades.

The obtained results may be used for identification of the elasticity modulus and for developing a flow stress model for numerical simulations of the steel continuous casting process.

Keywords: mechanical properties, rheological model, tensile test

W pracy przedstawiono badania właściwości wybranych gatunków stali w podwyższonych temperaturach. Wyniki przeprowadzonych badań wytrzymałościowych zostały przedstawione w pracy na wykresach i w tabeli. Pozwalają one na dokonanie matematycznego opisu wartości odkształcenia w zakresie plastycznym w zależności od zmiany wielkości stanu naprężenia w badanych gatunkach stali.

Otrzymane wykresy mogą być użyte do identyfikacji modułu sprężystości i do opracowania modelu naprężenia uplastyczniającego wykorzystywanych w symulacjach numerycznych procesu ciągłego odlewania stali.

1. Introduction

Steel slabs are cast in continuous casters which feature densely arranged roller pairs installed within consecutive segments. The strand forming in the mould is pulled out by motorised rolls. The total strand pulling force is the sum of pulling forces of all motorised rolls and must exceed the strand resistance force. A short stoppage of the machine causes an increase in the resistance force value by about 70%.

As a result of the pulling force impacting on the thin shell under the mould, the value of the total strain may exceed the limit strain value; and if the shell thickness is too small, it may cause its breakout. As a consequence steel leaks out of the liquid strand core, which in turn destroys one or more continuous caster segments and interrupts the steel casting process.

Strains also occur during the bending and straightening of the strand, and also the forming and eliminating of bulges between pairs of strand guiding rollers. This leads to internal cracks that occur after exceeding the plastic strain limit value in the vicinity of the crystallization front [1,2].

Due to difficulties related to the development of the research methodology, and the high costs of instrumentation to enable mechanical properties to be tested at high temperatures, the available references are short of data that would allow the determination of the limit value of plastic strain for the se-

lected steel grades near the crystallization front. Publications on this subject are very scarce [3], and mechanical tests of steel before or after mechanical working [4-7], along with tests of powder metallurgy products [8,9], are unsuitable for this purpose.

2. Tests of steel strength near to the solidus temperature

In order to reduce the strains caused by bulging, rollers that have as small a diameter and as minimal an axes span as possible, should be used. Strand bending and straightening effects are reduced by the use of multi-point bending and straightening, and the use of as large a caster radius as possible. The impact of the pulling force is decreased by increasing the number of drive rollers deployed at both sides of the strand that have been pulled out.

Results of such tests in industrial practice may be used to prevent a shell breakout and a leakage of the liquid core.

Tensile tests at high temperatures corresponding to the temperatures in the solidified shell in the zone under the mould are used to determine steel rheological properties, and are conducted by testing machines that are equipped with high temperature furnaces and extensometers. A testing machine, along with its accessories that was used for the tests, is presented in Fig. 1.

* AGH UNIVERSITY OF SCIENCE AND TECHNOLOGY, FACULTY OF METALS ENGINEERING AND INDUSTRIAL COMPUTER SCIENCE, AL. A. MICKIEWICZA 30, 30-059 KRAKÓW, POLAND

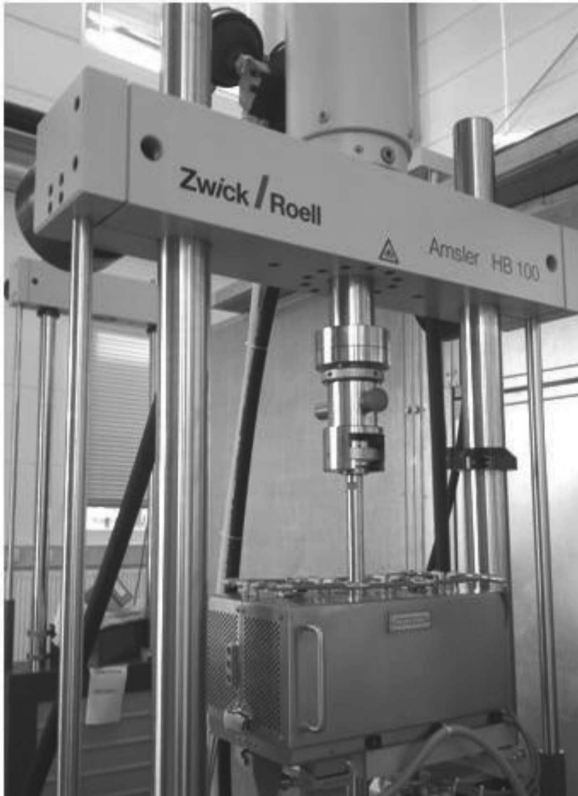


Fig. 1. A testing machine and a high temperature furnace for sample heating

The machine presented in Fig. 1 is equipped with a hydraulic cylinder that enables samples to be compressed and tensioned with a force not exceeding 100kN. To obtain such a high accuracy of measurements to be conducted at high temperatures, a tensometric head - enabling a force up to 5kN to be measured - was used. These tensile tests were performed in a protective argon atmosphere within the furnace. The samples tested were connected to the extensometer, with holders made of Al_2O_3 . The extensometer was used to make a precise measurement and to determine the elasticity modulus correctly.

3. Mechanical tests of selected steel grades at high temperatures

Static tensile tests were performed for 3 steel grades: S235JR, S320GD and UG-m. Their chemical compositions were determined with a compact optical emission spectrometer. The obtained results of steel chemical composition analysis are presented in Table 1.

The measurements were conducted at temperatures of 700, 1000, 1100 and 1150°C. This selected range corresponded to the temperature distribution at the strand surface in the zone under the mould. The samples tested had a cylindrical shape, with a diameter of 10 mm and a length of 120 mm. For tensile tests in the elastic range, the stress increment rate had to, pursuant to the applicable standards, range from 2 to 20N/mm²s. Above the elastic strain, the tensioning was conducted with a strain rate under 0.008s⁻¹. The changes in the stress values depending on the strain during the tensile tests are presented in Fig. 2.

TABLE 1

The chemical composition of the steel grades tested

Steel	Chemical composition [%]								
	C	Mn	Si	P	S	Cu	Cr	Ni	Mo
S235JR ¹⁾	0.08	0.52	<0.005	0.015	0.014	0.03	0.007	0.007	<0.005
S320GD ²⁾	0.09	0.74	0.02	0.013	0.01	0.02	0.02	0.07	0.007
UG-m	0.05	0.21	0.007	0.011	0.009	0.03	0.008	0.007	<0.005

¹⁾ acc. to PN-EN 10025-2:2007

²⁾ acc. to PN-EN 10346:2011

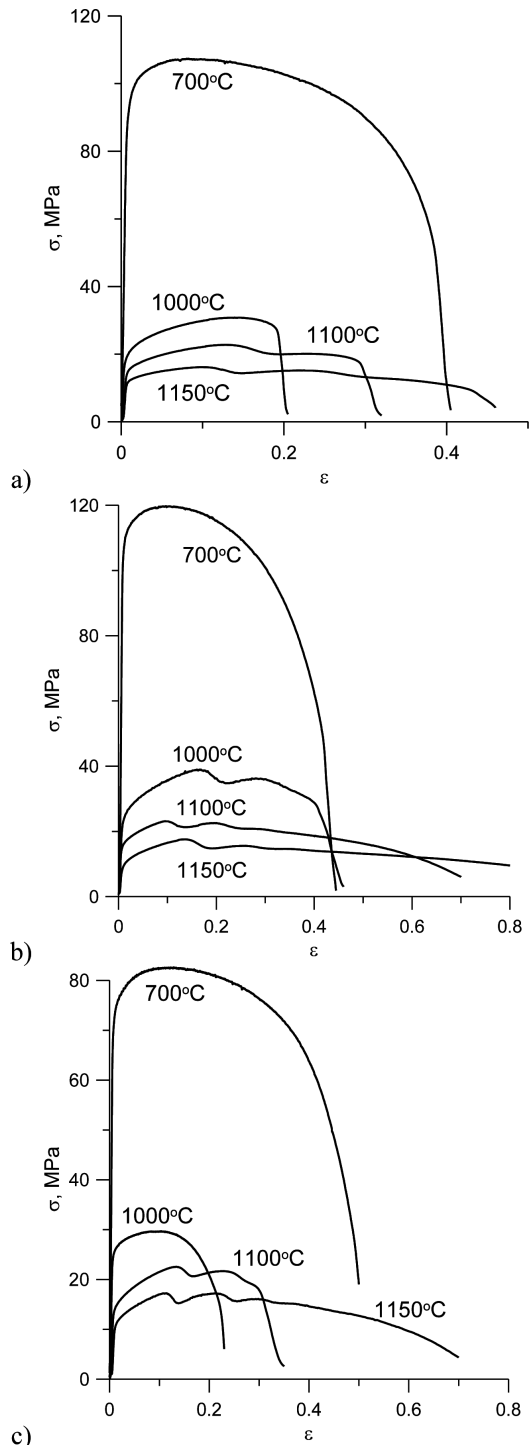


Fig. 2. Changes in stress values versus strain values for steels: a) S235JR, b) S320GD, c) UG-m

The results presented in Fig. 2 indicate that:

- as the temperature increases, the yield stress at which the material tested deforms plastically decrease,
- most of the recorded curves show a decrease in the flow stress for higher strain values, which is caused by the occurrence of recrystallization,
- as the temperature increases, the intensification of the recrystallization process causes an increase in plasticity, which may be observed as an increase in sample elongation,
- the nature of the recorded graphs indicates that despite so high temperatures of deformation elastic strain occurs.

The tests of strength properties of the selected steel grades have been used for the numerical modelling of stress and strain distribution inside solidifying strands below a continuous caster for slabs. An elasto-plastic rheological model with non-linear strain hardening was applied for the mathematical description of stress changes in relationship to the change in strain:

$$\sigma = \sigma_{\infty} + (\sigma_0 - \sigma_{\infty}) e^{-\alpha \cdot \varepsilon^{pl}} \quad (1)$$

where:

σ_0 – yield point,

σ_{∞} – limit stress,

α – strain hardening index,

ε^{pl} – plastic strain.

The estimated values of model parameters are presented in Table 2. The values of Young modulus E are also presented here.

TABLE 2

The rheological model parameter values (1) for steels: S235JR, S320GD and UG-m

Steel	T , °C	E , MPa	σ_0 , MPa	σ_{∞} , MPa	α
S235JR	700	175451.66	70.51	106.83	90.36
	1000	30534.68	19.18	39.48	22.00
	1100	12846.78	14.03	24.61	20.06
	1150	9245.21	7.55	18.40	17.68
S320GD	700	169366.47	97.25	119.54	55.32
	1000	26182.18	17.27	30.97	25.00
	1100	9486.83	13.29	23.31	21.44
	1150	7363.78	11.54	17.70	15.00
UG-m	700	223529.36	64.18	82.29	53.58
	1000	9938.54	24.01	29.81	37.60
	1100	8876.59	12.67	24.43	13.97
	1150	5838.82	9.72	21.50	10.00

The ProCAST window for defining the rheological model is presented in Fig. 3. It consists of a few tabs that enable the operator to enter the model parameter values, depending on the temperature.

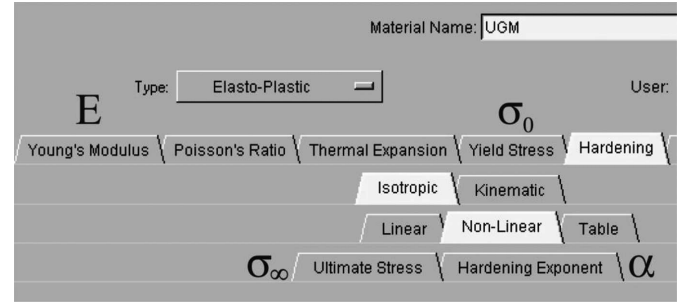


Fig. 3. The ProCast window for defining the elasto-plastic rheological model with a non-linear strain hardening

Implementing of the rheological model into the ProCast software requires the operator to complete a few tables in the graphic user interface (GUI). The use of this model allows them to carry out a simulation of stress and strain distribution in the solidified volume of the strand cast below a continuous caster.

4. Conclusion

As the temperature increases, the steel strength decrease, and at the solidus temperature it is very low. As a consequence a tensile stress growth in the forming shell may lead to the occurrence of internal cracks, or even to liquid core leakages. Therefore it is vital to determine those stress values which have exceeded the shell strength. This requires the testing of the rheological properties, and also to determine the susceptibility of the solidified shell to crack under the influence of the ferrostatic pressure in the zone below the mould.

The results of the conducted strength tests of the selected steel grades - which are presented herein in the graphs and in the table – allows us to describe mathematically the change in the stress value depending on the change in strain within the plastic range in the steel grades tested.

The determination of elongation of the tested samples allows the graphs to be used for the identification of the elasticity modulus, and for developing a flow stress model for numerical simulations of the steel continuous casting process [10-11].

Acknowledgements

The work is supported by the Ministry of Science and Higher Education (AGH agreement 11.11.110.293).

REFERENCES

- [1] M. Rywotycki, K. Miłkowska-Piszczyk, L. Trębacz, Identification of the boundary conditions in the continuous casting of steel, Archives of Metallurgy and Materials **57**, 1, 385-393 (2012).
- [2] K. Miłkowska-Piszczyk, M. Dziarmagowska, A. Buczek, J. Pióro, The methods of calculating the solidifying strand shell thickness in a continuous casting machine, Archives of Materials Science and Engineering **57**, 2, 75-79 (2012).
- [3] K.P. Sołek, L. Trębacz, Thermo-mechanical Model of Steel Continuous Casting Process, Archives of Metallurgy and Materials **57**, 1, 355-361 (2012).

- [4] X. Gui-Zhi, D. Hong-Shuang, Delayed Fracture Resistance and Mechanical Properties of 30MnSi High Strength Steel, *Journal of Iron and Steel Research International* **16**, 3, 49-54 (2009).
- [5] A.A. Hermas, I.M. Hassab-Allah, Microstructure, corrosion and mechanical properties of 304 stainless steel containing copper, silicon and nitrogen, *Journal of Materials Science* **36**, 14, 3415-3422 (2001).
- [6] D. Szelięga, J. Gawad, M. Pietrzyk, R. Kuziak, Inverse analysis of tensile tests, *Steel Research* **76**, 11, 807-814 (2005).
- [7] D. Kuc, V. Pidvysotsk'yy, R. Kuziak, Model zmian naprężenia uplastyczniającego i struktury w warunkach odkształcenia plastycznego na gorąco stali austenitycznej, *Hutnik-Wiadomości Hutnicze* **LXXVI**, 8, 604-607 (2009).
- [8] J. Karwan-Baczewska, M. Rosso, Effect of boron on microstructure and mechanical properties of PM sintered and nitrided steels, *Powder Metallurgy* **44**, 3, 221-227 (2001).
- [9] J. Karwan-Baczewska, T. Dymkowski, J.R. Sobiecki, T. Formąński, Processing and surface properties of based on iron sintered alloys after plasma nitriding treatment, *Archives of Metallurgy and Materials* **55**, 2, 383-389 (2010).
- [10] M. Knap, J. Falkus, A. Rozman, J. Lamut, The prediction of hardenability using neuronal networks, *Archives of Metallurgy and Materials* **53**, 3, 761-766 (2008).
- [11] A. Burbelko, J. Falkus, W. Kapturkiewicz, K. Sołek, P. Drożdż, M. Wróbel, Modeling of the grain structure in the steel continuous ingot by CAFE method, *Archives of Metallurgy and Materials* **57**, 1, 379-384 (2012).